# $^{35}$Cl Nuclear Quadrupole Relaxation in Antimony Trichloride

Noriaki Okubo and Yoshihito Abe

Institute of Physics, University of Tsukuba, Tsukuba, 305 Japan

Z. Naturforsch. **49a,** 680–686 (1994); received March 14, 1994

The $^{35}$Cl NQR frequency and spin-lattice relaxation time in $SbCl_3$ have been measured between 10 K and the melting point. The relaxation at low temperatures is attributed to the Raman process. A Debye temperature of 141 K and covalencies 0.390 and 0.356 are obtained. The latter values correspond well to those obtained from the NQR frequencies. For the relaxation above 200 K two more mechanisms are considered.

*Key words:* Antimony trichloride; Nuclear quadrupole relaxation; Raman process; Debye temperature; Covalency.

## 1. Introduction

Nuclear quadrupole relaxation, if it is proportional to $T^2$ at high temperatures, has often been attributed to the Raman process. The theory of nuclear quadrupole relaxation due to the Raman process was first developed for ionic crystals [1] and later extended to cases including covalency [2]. In [3] we have reported that the nuclear relaxation in niobium pentahalides ($NbCl_5$ and $NbBr_5$) can to some extent be explained by the latter theory, which assumes equivalence of the ions and axial symmetry about the bond. Those pentahalide-crystals, however, consisting of dimers, involve nonequivalent (terminal and bridging) halogen ions and non-axially-symmetric $p_\pi - d_\pi$ bonds. This was regarded as the reason for the remaining discrepancy between experiment and theory. Thus it was of interest to study the relaxation in substances satisfying the above assumptions of the theory.

Antimony trichloride ($SbCl_3$) should suit this purpose, because it does involve neither bridging nor $p_\pi - d_\pi$ bonds. The crystal structure [4, 5] belongs to the orthorhombic system, space group Pnma. The unit cell contains four equivalent monomers. Although the three chlorine atoms of a monomer occupy nonequivalent sites, one site I ($Cl_I$) and two site II ($Cl_{II}$), the difference in their environment is much smaller than in the niobium halides. Moreover, for chlorine nuclei having spin $I = 3/2$, the spin-lattice relaxation time $T_1$ can be determined uniquely. $^{35,37}$Cl NQR of $SbCl_3$ has been reported by many authors [6–15]. However, these studies are limited to temperatures below 180 K or above room temperature, and do not deal with $T_1$. The NQR was also reported for the $^{121,123}$Sb nuclei [6, 10, 16–20], however the spins being 5/2 and 7/2, the relaxation is governed by several $T_1$'s, and it is not easy to separate them uniquely. Besides, since in $SbCl_3$ an Sb atom is bonded to two types of Cl atoms at different distances, the theory of [1, 2] cannot be applied to the Sb nuclei. Since the resonance frequencies of Sb and Cl nuclei differ much, there is no interaction between their relaxation, and in this paper we have studied the chlorine NQR.

## 2. Experimental

$SbCl_3$ (Wako Pure Chemical) was used without further purification. The purity is stated to be higher than 99%. About 15 g of $SbCl_3$ were sealed in a pyrex ampoule with a small amount of helium gas, and then the sample was annealed. In high purity samples, supercooling down to temperatures several tens of a degree below the melting point ($T_m = 346.6$ K) was reported [21, 22]. We also observed supercooling by more than forty degrees. The measurement of $^{35}$Cl NQR was done at thermal equilibrium, which was reached after 30′. The temperature was regulated within 0.1 K and measured with a gold-iron vs. chromel thermocouple below room temperature and a copper vs. constantan one above it.

The $^{35}$Cl NQR was observed with a pulse spectrometer (Matec, Inc.). The spin echo signal after 90° –

---

Reprint request to Dr. N. Okubo, Institute of Physics, University of Tsukuba, Tsukuba, 305 Japan.

0932-0784 / 94 / 0600-0680 $ 06.00 © – Verlag der Zeitschrift für Naturforschung, D-72072 Tübingen

180° pulses was monitored. At every temperature the tuning was adjusted to optimize the signal. The signal-to-noise ratio of $^{35}$Cl nuclei was typically 60 for site I at 77 K, after 8 times averaging. $T_1$ was measured by applying another 90° pulse at a time $t$ in advance and measuring the echo height as a function of $t$. By the least-squares-method the recovery curve could be fitted with a single exponential function within a few %.

The whole system was controlled through a General Purpose Interface Bus (IEEE-488) line, and the measurement was carried out automatically using a program developed for the present purpose.

## 3. Results

The $^{35}$Cl NQR spectrum of SbCl$_3$ consists of two lines around 20 MHz. The intensity of the high frequency line is about half that of the low frequency line. The corresponding $^{37}$Cl NQR lines were also observed. The frequencies $\nu_Q$ agree with those reported in [6–14]. While the $\nu_Q$ of the high frequency line exhibits the usual negative temperature dependence, that of the low frequency line exhibits a much smaller dependence and below 45 K even a slightly positive dependence [10].

Figure 1 shows the temperature dependence of $T_1$ ($^{35}$Cl). Below 20 K, $T_1$ is too long to be measured exactly. $T_1$ at 10 K was estimated to be of the order of $10^3$ sec. This indicates that the value of $T_1$ is intrinsic and not shortened by magnetic impurities down to such low temperatures. Above 20 K the slope in the log-log plot becomes progressively gentler and approaches $-2$, whereas above 200 K it begins to become steeper again. Also, the signal intensity decreased up to 200 K proportional to $T^{-1}$, whereas above 200 K the decrease became progressively steeper toward $T_m$. A phase transition was reported for SbCl$_3$ [23]. Brown et al. observed an increase of the line width above room temperature, followed by a sudden drop at 342 K [12]. However the transition point $T_t$ is only a few degrees below $T_m$ and the signal became too week for an exact determination of $\nu_Q$ and $T_1$ there.

The ratio $T_1^{-1}$ ($^{37}$Cl)/$T_1^{-1}$ ($^{35}$Cl) was 0.69 for site I and 0.72 for site II, at 77 K. Unlike for bromine nuclei, the squared ratio of the magnetic moments $\mu$, $[\mu(^{37}\mathrm{Cl})/\mu(^{35}\mathrm{Cl}]^2 = 0.69$, is not so different from that of the quadrupole moments $Q$, $[Q(^{37}\mathrm{Cl})/Q(^{35}\mathrm{Cl})]^2 = 0.62$, and the ratio of $T_1^{-1}$ involves an error of 10%. Thus it is difficult to say, by comparing these ratios, whether the relaxation is dominated by magnetic or quadrupolar interaction. On the other hand, $T_1^{-1}(\mathrm{Cl_I})/T_1^{-1}(\mathrm{Cl_{II}})$ at given temperatures is close to $[\nu_Q(\mathrm{Cl_I})/\nu_Q(\mathrm{Cl_{II}})]^2$ for the respective nuclear species. This suggests that the quadrupolar interaction is dominant.

For the $^{35}$Cl nucleus, $T_2$ was 1.5 ms for site I and 1.8 ms for site II, and $T_2^*$ was 70 μs for site I and 80 μs for site II, typically at 77 K.

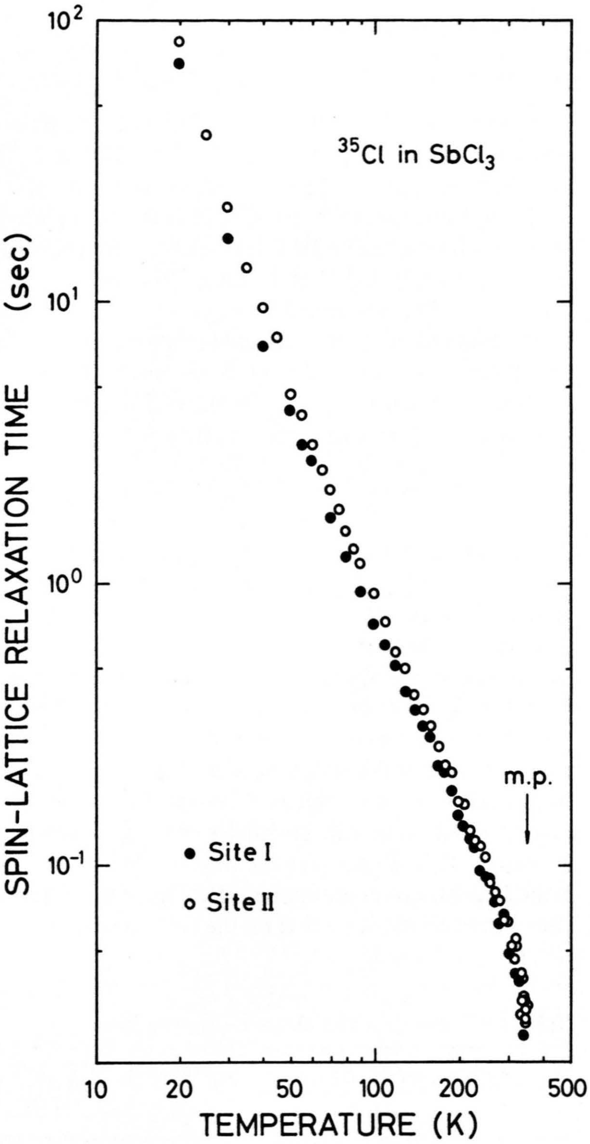

Fig. 1. Temperature dependence of the spin-lattice relaxation time $T_1$ of $^{35}$Cl nuclei in SbCl$_3$.

## 4. Analysis and Discussion

### *4.1 Frequency*

In the unit cell of $SbCl_3$, four chlorine atoms occupy site I and eight site II, as shown in Figure 2 [5]. The bond lengths $a$ of Sb–Cl at the two sites are given in Table 1. From the observed ratio of the signal intensities, therefore, the NQR line of higher frequency was assigned to $Cl_I$ and that of lower frequency to $Cl_{II}$ nuclei [24]. This assignment is consistent with the usually observed fact that, as covalency increases, the NQR frequency rises and the bond length shortens.

The dependence of $\nu_Q(^{35}Cl)$ on temperature $T$ can approximately be expressed by the polynomial

$$\nu_Q(T) = a_{-1}T^{-1} + a_0 + a_1 T + a_2 T^2. \tag{1}$$

The coefficients are given in Table 2. The temperature dependence of $\nu_Q(Cl_{II})$ is by a factor 1/5 smaller than that of $\nu_Q(Cl_I)$.

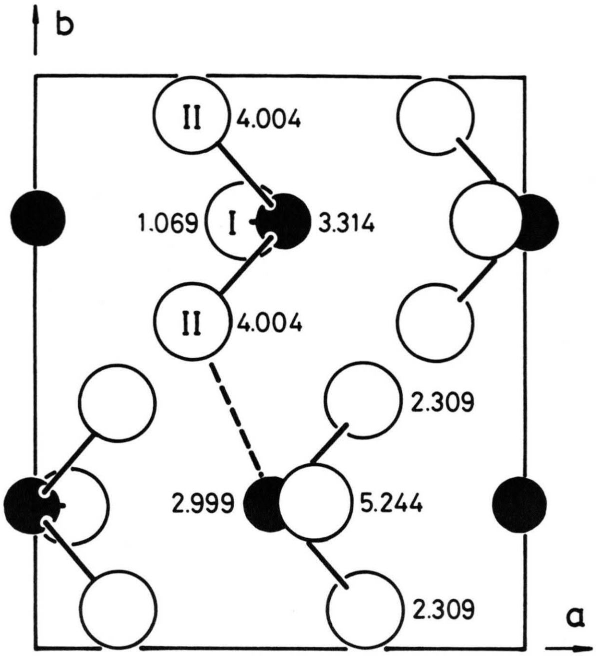

Fig. 2. The unit cell of $SbCl_3$ [5]. Closed circles represent Sb atoms and open ones Cl atoms, for which two sites are shown by the letters I and II. The $z$ values of the atoms are given in Å. The intermolecular bonding is denoted by the broken line.

In Fig. 2, the distance 3.457 Å between $Cl_{II}$ and Sb of the adjacent molecule is smaller than the sum of the van der Waals radii (4.0 Å) [5]. If in addition to the intramolecular bond of Cl with Sb some intermolecular bonding is assumed, the difference between $\nu_Q(Cl_{II})$ and $\nu_Q(Cl_I)$, the large values of the asymmetry parameter $\eta$ at $Cl_{II}$ and the Sb nuclei can be reasonably explained [25]. Following the analysis of the Sb–Br bond in pentabromoantimonate(III) [26], if the effect of the intermolecular bonding on the EFG is assumed to be $\chi$ times the EFG along the primary bond, and the angle between these bonds is denoted by $\phi$, then $\eta$ $(Cl_{II})$ can be expressed as a function of $\chi$ and $\phi$. Since the average $\eta$ $(Cl_{II})$ is reported to be 0.15 [9, 11, 14, 25] and $\phi$ is calculated to be 106.9° [5], we can solve the relation for $\chi$ to obtain a value of 0.106. Then the EFG's along the primary and intermolecular bonds are 1.037 and 0.110 times the largest component of the composed EFG, respectively.

Table 1. Crystal data and chlorine coupling constant.

| $N$ | $V$(Å$^3$) | $a$(Å) [5] | | $d$(g/cm$^3$) | $e^2Qq_{at}/h$ (MHz) [28] |
|---|---|---|---|---|---|
| | | I | II | | |
| 16 | 482.3 | 2.340 | 2.368 | 3.141 | 109.74 |

Table 2. Expansion coefficients of $\nu_Q(T)$ and standard deviation $\sigma$.

| Coefficient and $\sigma$ | Site I | Site II |
|---|---|---|
| $a_{-1}$/MHz · K | $-9.65482 \cdot 10^{-1}$ | $6.54899 \cdot 10^{-2}$ |
| $a_0$/MHz | 21.0507 | 19.3003 |
| $a_1$/MHz · K$^{-1}$ | $-1.47530 \cdot 10^{-2}$ | $2.07238 \cdot 10^{-4}$ |
| $a_2$/MHz · K$^{-2}$ | $-2.26217 \cdot 10^{-6}$ | $-2.11612 \cdot 10^{-6}$ |
| $\sigma$ (MHz) | $1.27650 \cdot 10^{-3}$<br>59 data<br>(20 to 340 K) | $7.62003 \cdot 10^{-4}$<br>74 data<br>(20 to 345 K) |

Chihara et al. attributed also the small temperature dependence of $\nu_Q(Cl_{II})$ to the intermolecular bonding [10]. The resulting positive temperature dependence was considered to out-weigh most of the usual negative one. However, part of the difference between the temperature dependences of the two sites may also be attributed to the difference in the effectiveness of the librations in averaging the EFG, arising from the difference in the angles between the libration axes and the principal $z$ axis.

Bond fluctuation was proposed to explain the Raman spectra [27]. However, the effect on the NQR, if any, will enter $\nu_Q$ and $T_1$ only as averaged because of the rapid transfer of electrons.

### 4.2 *Relaxation Due to the Raman Process*

The approach with increasing temperature to a $T^2$ dependence of the relaxation rate suggests the presence of the Raman process. On the other hand, the increase of the temperature dependence above 200 K up to $T_m$ suggests the presence of still another relaxation mechanism. First the contribution of the Raman process shall be discussed. For convenience we follow the notation used in [1–3], but with a few modifications to avoid confusion.

In the case of spin 3/2, the expression for $T_1^{-1}$ due to the process is derived in [3]:

$$T_1^{-1} = \frac{3\,e^4 Q^2 \langle r^{-3}\rangle_{\rm H}^2 c^3}{100\,\pi^3 a^7 d^2 v_s^3} \cdot T^{*2} \sum_{\nu=1}^{4} (N_{1\nu} + 4\,N_{2\nu})\, D_\nu(T^*), \tag{2}$$

where $d$ denotes the density of the crystal, $T^*$ the temperature divided by the Debye temperature $\theta_D$ $r$ the interionic distance and $\langle\ \rangle_{\rm H}$ means the expectation value with respect to the valence $p$ electron of the halogen ion. $c$ is defined as $c = k_D\, a$ with the maximum wave number $k_D = (6\pi^2 N/V)^{1/3}$, $N$ being the number of atoms in the unit cell of volume $V$. The sound velocity $v_s$ is related with $\theta_D$ by

$$\hbar\,\omega_D = \hbar\,v_s\,k_D = k_B\,\theta_D, \tag{3}$$

where $\omega_D$ is the Debye frequency and $k_B$ the Boltzmann constant.

In [3] the expressions for $N_{\mu\nu}$ $(\mu = 1, 2)$ were derived for the halogen nuclei of the $MX_5$ type transition metal halides with dimeric structure. Since, if intermolecular bonding is neglected in $SbCl_3$, each Cl atom is bonded to a single Sb atom, the expressions for the terminal halogen atoms in the $MX_5$ compound can be applied. That is

$$N_{11} = N_{12} = 4\lambda^2 \left(1 - \frac{a\,\lambda'}{\lambda}\right)^2, \tag{4}$$
$$N_{13} = N_{14} = 0,\quad N_{21} = N_{22} = \lambda^2,\quad N_{23} = N_{24} = 0,$$

where $\lambda$ is a measure of a degree of covalency and $\lambda'$ its first derivative with respect to $r$. $D_\nu(T^*)$ is defined as

$$D_\nu(T^*) = T^* \int_0^{1/T^*} \frac{x^2 e^x}{(e^x - 1)^2}\, L_\nu(c\,T^* x)\, dx, \tag{5}$$

where $x = \hbar\,\omega/k_B T$, $\omega$ being the angular frequency of the phonon. Since $N_{\mu 3}$ and $N_{\mu 4}$ vanish, only the following $L_\nu(k\,a)$ are needed:

$$\begin{aligned} L_1(k\,a) &= \{S_1^2\}_{\boldsymbol{k}}^2 = \{\tfrac{1}{2} - \tfrac{1}{2} f(2\,k\,a)\}^2, \\ L_2(k\,a) &= \{C_1^2\}_{\boldsymbol{k}}^2 = \{\tfrac{3}{2} - 2 f(k\,a) + \tfrac{1}{2} f(2\,k\,a)\}^2, \end{aligned} \tag{6}$$

where

$$S_n = \sin(a\,\boldsymbol{k} \cdot \boldsymbol{n}),\quad C_n = \cos(a\,\boldsymbol{k} \cdot \boldsymbol{n}) - 1,$$
$$f(y) = \frac{\sin y}{y}, \tag{7}$$

and $\{\}_{\boldsymbol{k}}$ means the average about the direction of $\boldsymbol{k}$, $\boldsymbol{k}$ being the wave vector of the phonon, $k$ its magnitude and $\boldsymbol{n}$ the unit vector from the halogen ion to the metal one.

### 4.3 *Estimation of Debye Temperature*

Introducing a scaling time $\tau$ defined as

$$\tau^{-1} = \frac{3\,e^4 Q^2 \langle r^{-3}\rangle_{\rm H}^2 c^3}{100\,\pi^3 a^7 d^2 v_s^3} (N_{11} + 4\,N_{21}), \tag{8}$$

we can reduce (2) to the form

$$(T_1\,T^2)^{-1} = (\tau\,\theta_D^2)^{-1} [D_1(T^*) + D_2(T^*)]. \tag{9}$$

Then, by fitting (9) to the experimental result, we can determine $\theta_D$ together with $\tau$ as fitting parameters. The integration of (5) was carried out numerically. The least-squares-fitting was performed for the range from 20 K to 190 K by assuming a common $\theta_D$ for the two sites. The results are shown in Fig. 3 and Table 3.

The Debye temperature for $SbCl_3$ is not reported, but it may be estimated from the diagonalized coefficients $B_{ij}$ in the temperature factor of the X-ray analysis [5]. The estimated values are 84.8 K to 116.2 K for $Cl_I$ and 72.6 to 115.5 K for $Cl_{II}$, while 106.1 to 121.2 K for Sb, depending on the directions of the principal axes. They are low compared with 141.2 K obtained from $T_1$. At room temperature, where the X-ray analysis was possibly done, the temperature factor may be affected by thermal motions becoming active toward $T_m$. For $v_s$, we obtain a value of $1.476 \cdot 10^5$ cm/sec.

### 4.4 *Estimation of Covalency*

Now we can estimate $\lambda$ from the $\tau$ using (8) with (4). The $e^2 Q \langle r^{-3}\rangle_{\rm H}$ is given by $(5/4)\, e^2 Q\, q_{at}$, $e^2 Q\, q_{at}$ being the quadrupole coupling constant for the free atom. The value of $e^2 Q\, q_{at}$, obtained from the atomic

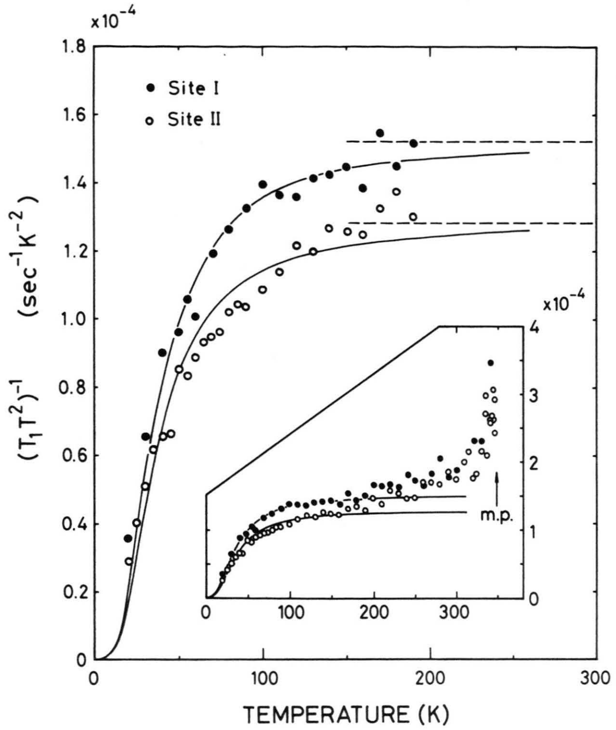

Fig. 3. The result of a least-squares-fitting of (9) to the data up to 190 K for the two sites of Cl atoms in SbCl$_3$. The broken lines represent the asymptotes at high temperatures. The inset shows the temperature dependence of $(T_1 T^2)^{-1}$ up to the melting point.

Table 3. Debye temperature $\theta_D$ and scaling time $\tau$.

| Site | $\theta_D$(K) | $\tau$ (sec) |
|---|---|---|
| I | 141.2 | 0.1616 |
| II | | 0.1992 |

Table 4. Two measures of covalency, $\lambda$ and $f$.

| Compound | Site | $\lambda$ | $f$ |
|---|---|---|---|
| SbCl$_3$ | I | 0.390 | 0.387 |
| | II | 0.356 | 0.355 |
| NbCl$_5$ | ax | 0.145 | 0.133 |

beam experiment, is given in Table 1 [28]. The crystal structure and the atomic positions are definitely determined for SbCl$_3$ [5, 29]. $c = k_m a$ is calculated to be 2.931 for site I and 2.966 for site II from the data in Table 1. The relation

$$\lambda \propto \exp(-r/\varrho) \tag{10}$$

was assumed after Yosida and Moriya [2]. For the repulsive range parameter $\varrho$ [30], hence for the inverse of $-\lambda'/\lambda$ involved in $N_{11}$, a value of 0.345 Å [2] was again employed. Then we obtain the values of $\lambda$ in Table 4. In the table the result for NbCl$_5$ [3] is also listed for comparison.

$\lambda$ is defined as the amount of p electron which is transferred from the halogen ion to the metal ion in forming covalent bonding and is supposed to produce the EFG with the largest component along the bond [2]. It just corresponds [31] to the number of unbalanced p electrons, $f$, defined as

$$f = \frac{e^2 Q q_{\mathrm{mol}}}{e^2 Q q_{\mathrm{at}}}, \tag{11}$$

where $e^2 Q q_{\mathrm{mol}}$ is the coupling constant for the molecule and related with the resonance frequency $\nu_Q$ by

$$\nu_Q = \frac{e^2 Q q_{\mathrm{mol}}}{2h} \left(1 + \frac{\eta^2}{3}\right)^{1/2}. \tag{12}$$

Thus, we can compare $\lambda$ determined from $T_1$ with $f$ determined independently from $\nu_Q$. Values of 0 ~ 0.06 are reported for $\eta$ (Cl$_{\mathrm{I}}$) and 0.14 ~ 0.16 for $\eta$ (Cl$_{\mathrm{II}}$) [9, 11, 14, 25]. Since $\lambda$ means the static value, $e^2 Q q_{\mathrm{mol}}$ should also be calculated from the static frequency $\nu_Q$ not involving the thermal effect. This effect may be properly corrected for by using the value obtained by extrapolating to 0 K the asymptote of the $\nu_Q(T)$ curve at high temperatures, in accordance with the Bayer theory [28]. The estimated values of $\nu_Q$ are 21.3 MHz for site I and 19.5 MHz for site II. The result for $f$ is also listed in Table 4.

### 4.5 *Remarks on $\lambda$ and $f$*

The agreement between $\lambda$ and $f$ in Table 4 is surprisingly good. However, these values should not be taken literally, for they involve some ambiguities. When the fitting is performed with assuming different $\theta$'s for the sites, we obtain by several % lower and higher $\theta$'s for sites I and II, respectively. Correspondingly, we obtain $\lambda$'s more than ten % lower and higher than those in Table 3. In Figure 3, however, even below 190 K the curve for site II seems to be influenced by another mechanism dominant at high temperatures. In the temperature factor, the larger values involved in the diagonalized $B_{ij}$ for site II may be related with this fact.

In obtaining the value for $f$ in Table 4, the contribution from the intermolecular bonding was neglected. If it is taken into consideration, we obtain a value of 0.368 for $f$ of the primary bond of $\mathrm{Cl_{II}}$ and similarly 0.039 for $f$ of the intermolecular bond. However, the values of $\lambda$ to be compared with these cannot be obtained from the theory [2], which assumes equivalence of the ions. The derivation of the expression for the case including ions at different distances is complicated.

Furthermore, we have neglected the anharmonic Raman (aR) process [32]. In ionic crystals the first order Raman (1R) process just considered could not bring about sufficient relaxation, and the aR process was invoked. The contribution to the relaxation cannot be discriminated in the temperature dependence from that due to the 1R process. For $\mathrm{SbCl_3}$ a low Grüneisen constant is reported [33], but the information is not sufficient to estimate the magnitude of the latter contribution. If it cannot be neglected, the present values of $\lambda$ will become smaller.

Thus, although the fine agreement between $\lambda$ and $f$ may be accidental, a substantial agreement nevertheless exists. This is also supported by the comparison with $\mathrm{NbCl_5}$ in Table 4. The change of $f$ is associated with a corresponding change of $\lambda$. In molecular crystals there may be such mechanism that the 1R process alone can explain the experimental result.

### 4.6 High Temperature Region

The contribution to $T_1^{-1}$ from mechanisms other than the Raman process is given by subtracting the latter contribution from the experimental $T_1^{-1}$. When the logarithm of the remaining part was plotted versus $1/T$, a bending line with a steep slope at small $1/T$ and a gentle slope at large $1/T$ was obtained. So the curve was fitted by two exponential terms:

$$(T_1^{-1})_{\mathrm{exp}} - \left(\frac{T^2}{\tau\,\theta_{\mathrm{D}}^2}\right)[D_1(T^*) + D_2(T^*)] = a \exp\left(-\frac{E_a}{RT}\right) + b \exp\left(-\frac{E_b}{RT}\right). \tag{12}$$

For $E_a$ and $E_b$, values of $8 \pm 2$ and $50 \pm 10$ kJ/mol were obtained, respectively, for either site. The former activation energy may be attributed to rotational motions about the axes of the moment of inertia, and the latter to tumbling or diffusive motions leading the melting. Brown et al. reported an activation energy of 140 kJ/mol from an Arrhenius plot of the conductivity data [12].

Alternatively, the deviation from the temperature dependence corresponding to the Raman process may be attributed to the softening [34] accompanying the phase transition reported at 342 K. Since (2) predicts for $T_1^{-1}$ a dependence of $\omega_{\mathrm{D}}^{-5}$, a softening of 16% is then obtained for $\omega_{\mathrm{D}}$ at $T_t$. Fontana et al. reported a small decrease of the frequency for a librational mode toward $T_m$ [21]. The softening may also contribute to the temperature dependence of $\nu_Q$ [34].

## 5. Conclusion

The $^{35}$Cl NQR frequency and the spin-lattice relaxation time in $\mathrm{SbCl_3}$ have been measured between 10 K and the melting point. The relaxation at lower temperatures was analyzed quantitatively by the theory of the Raman process. A good correspondence of the covalency estimated from the relaxation to that calculated from the NQR frequency was again obtained. In molecular crystals, Yosida and Moriya's theory seems to predict the correct magnitude to the nuclear quadrupole relaxation due to the Raman process.

[1] J. Van Kranendonk, Physica **20,** 781 (1954).
[2] K. Yosida and T. Moriya, J. Phys. Soc. Japan **11,** 33 (1956).
[3] N. Okubo, H. Sekiya, C. Ishikawa, and Y. Abe, Z. Naturforsch. **47 a,** 713 (1992).
[4] I. Lindqvist and A. Niggli, J. Inorg. Nucl. Chem. **2,** 345 (1956).
[5] A. Lipka, Acta cryst. **B 35,** 3020 (1979).
[6] H. G. Dehmelt and H. Krüger, Z. Phys. **130,** 385 (1951).
[7] T. C. Wang, Phys. Rev. **99,** 566 (1955).
[8] S. Ogawa, J. Phys. Soc. Japan **13,** 618 (1958).
[9] T. Okuda, A. Nakao, M. Shiroyama, and H. Negita, Bull. Chem. Soc. Japan **41,** 61 (1968).
[10] H. Chihara, N. Nakamura, and H. Okuma, J. Phys. Soc. Japan **24,** 306 (1968).
[11] K. V. Raman, R. Jagannathan, and R. T. Narasimhan, J. Chem. Phys. **59,** 792 (1973).
[12] R. J. C. Brown, G. C. Gillies, R. E. Halliwell, and S. Segel, J. Mag. Resonance **20,** 286 (1975).
[13] Y. E. Sapozhnikov and Y. B. Yasman, Izv. Akad. Nauk SSSR Ser. Fiz. **42,** 2148 (1978).
[14] D. Giezendanner, S. Sengupta, and E. A. C. Lucken, J. Mol. Struct. **58,** 229 (1980).
[15] S. J. Melnick and M. A. Whitehead, J. Mol. Struct. **116,** 217 (1984).

[16] V. S. Grechishikin and I. A. Kyuntsel, Sov. Phys. Solid State **5,** 694 (1963).

[17] V. S. Grechishikin and A. D. Gordeev, Optics and Spectroscopy **18,** 96 (1965).

[18] V. S. Grechishikin and E. M. Shishkin, Sov. Phys. Solid State **11,** 730 (1969).

[19] N. E. Ainbinder, V. S. Grechishikin, A. D. Gordeev, and A. N. Osipenko, Sov. Phys. Solid State **10,** 1592 (1969).

[20] A. S. Azheganov, N. E. Ainbinder and Y. I. Manzhura, Sov. Phys. Solid State **17,** 1013 (1975).

[21] M. Fontana, G. Maisano, N. Micali, P. Migliardo, C. Vasi, and F. Wanderlingh, Optica Acta **27,** 1087 (1980).

[22] F. Aliotta, G. Maisano, N. Micali, P. Migliardo, C. Vasi, and F. Wanderlingh, J. Chem. Phys. **76,** 3987 (1982).

[23] W. M. C. Julien and H. Gerding, Rec. Trav. Chim. Pays Bas **91,** 743 (1972).

[24] The numbering of the sites in the present paper agrees with that in [4] and [5]. In [10], the interchanged numbers are used.

[25] G. E. Peterson, Thesis, University of Pittsburgh (1962).

[26] H. Ishihara, S. Dou, and A. Weiss, Ber. Bunsenges. Phys. Chem. **95,** 659 (1991).

[27] H. Friedwold and W. Brockner, Z. Naturforsch. **46a,** 595 (1991).

[28] T. P. Das and E. L. Hahn, Nuclear Quadrupole Resonance Spectroscopy, Solid State Physics, F. Seitz and D. Turnbull (Academic Press, New York 1958) Supplement 1.

[29] B. F. Bowles, G. T. Scott, and S. E. Babb, Jr., J. Chem. Phys. **39,** 831 (1963).

[30] C. Kittel, Introduction to Solid State Physics, 6th ed., p. 71.

[31] In Eq. (4.7) of [2], $\lambda_n$ has a meaning of the weight for covalency through $\sigma$-bond with the $n$-th atom on the $\zeta$ axis. If $\pi$-bond through $p_\xi$ and $p_\eta$ orbitals is explicitly supposed with keeping axial symmetry along the bond, (4.7) is multiplied by $-1/2$ through the procedure to obtain (4.6). In addition, hybridization of s orbital with the amount of $\alpha$ is included, $\lambda_n$ should be replaced by $(1-\alpha^2)\,\sigma-\pi/2$, where $\sigma$ and $\pi$ denote the amounts of $\sigma$- and $\pi$-bond characters, respectively. Since then $f$ is also given by $(1-\alpha^2)\,\sigma-\pi/2$, $\lambda_n$ is to be compared just with $f$. In [2] $\lambda_n$ is later written as $\lambda$, by assuming the equivalence of the ions.

[32] J. van Kranendonk and M. B. Walker, Canad. J. Phys. **46,** 2441 (1968).

[33] N. E. Ainbinder and A. S. Azheganov, J. Mol. Struct. **83,** 93 (1982).

[34] H. M. Van Driel, M. Wiszniewska, B. M. Moores, and R. L. Armstrong, Phys. Rev. **B6,** 1596 (1972).